Numerical Calculation of the Dynamic Behavior of Asynchronous Motors with COMSOL Multiphysics

J. Güdelhöfer, R. Gottkehaskamp and A. Hartmann
Department of Electrical Machines and Electromagnetic Field Theory, University of Applied Sciences Düsseldorf, Düsseldorf, Germany

Abstract: This paper shows how a time-dependent and non-linear simulation of the dynamic operation behavior of an induction machine is executed by means of the "Rotating Machinery" interface from COMSOL Multiphysics 4.2a. The two-dimensional FEM model is connected to electrical circuits by coupling the physics "Rotating Machinery" and "Electrical Circuit" interfaces. These circuits include the lumped electrical components to simulate the electrical effects in the end area as well as the three-phase-voltage system to supply the stator.
Simulations are made for constant slip values as well as dynamical start-up with an additionally defined equation of motion as an ordinary differential equation by means of the "Global ODEs and DAEs" interface.

Keywords: Asynchronous Machines, Dynamic Behavior, Lumped Components

1. Introduction

The numerical electromagnetic field calculation is an important tool to calculate and design electrical machines. To lay out a design for the magnetic circuit it is sufficient to consider two dimensions, where leakage inductances and resistances, caused by winding overhangs and short-circuit rings of an Induction Motor in the end area, are neglected.
However, if the stationary and dynamical operating behavior are to be simulated, magnetic and electric influences have to affect the model simultaneously. In three-dimensional simulations, winding overhangs and short-circuit rings can be represented geometrically and therefore also be considered in calculations, but the solving times for these exact models are unacceptably high. The effects on the operating behavior can be considered very accurately in less time consuming two-dimensional calculations [1][2], by simulating the electromagnetic conditions in the end area of the machine via lumped components coupled to the FEM model.
Numerical models of electrical machines are often supplied with impressed current densities. This alternative allows the calculation of the static magnetic circuit. For stationary and dynamical simulations, it has to be considered that the RMS values and the time dependence of the phase currents adapt according to the amount of revolutions per minute, the magnetic saturation, and the applied voltage. However, this is only possible if the stator is also connected to a voltage system.

2. Modeling

An asynchronous machine (ASM) basically consists of a stator and a rotor, both commonly being made of laminated iron cores.
When supplied with a three-phase-voltage system, a three-phase-winding in the stator causes a rotating magnetic field. If this time-dependent field rotates relative to the rotor, it induces electrical fields in either the rotor windings or in a rotor circuit cage, which impells current flows in the direction of the electrical fields. The direction of these induced currents is basically the opposite of the inducing currents (Lenz's law), generating magnetic poles in the rotor which then follow the rotating field and simultaneously produce a torque.

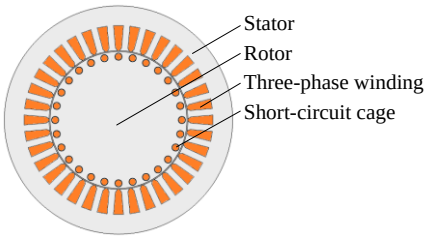

Figure 1. FEM geometry of an asynchronous machine

A general 2D FEM geometry for an induction machine is shown in Figure 1. The modeling theory to consider the electrical effects in the end room in two dimensional simulations is taken from [1] and [2]. Summed up, if a short circuit cage is used, the short circuit ring is replaced by a resistor and an inductor between two rotor bars and one resistor for the part of the rotor bar

which is not inside the iron anymore but in the ring (Figure 2).

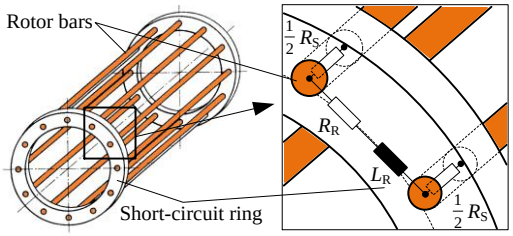

Figure 2. The Short-circuit ring is being replaced with lumped elements.

The effects of the magnetic leakage fluxes of the winding overhangs in the stator are considered as inductors in the stator circuit, which also contains the phase resistors. Methods to calculate these lumped elements can be found in [2].

3. Use of COMSOL Multiphysics

3.1 General FEM Model

The FEM model is built within the Rotating Machinery physic where the general equations

$$\kappa\frac{\partial \vec{A}}{\partial t}+\vec{\nabla}\times\vec{H}-\kappa\vec{v}\times\vec{B}=\vec{J} \qquad (1)$$

and

$$\vec{B}=\vec{\nabla}\times\vec{A} \qquad (2)$$

are solved. Domains for the stator slots are defined as Multi Turn Coil Domains and are not affected by the skin effect leading to errors for windings with big wire cross-sections. Rotor bars are defined as Single Turn Coil Domains and are affected by the skin effect. Since the stator and the rotor domains are made of non-linear iron, H(B)-functions need to be defined for both. An alternative is to define functions for the relative permeabilities for the domains.

3.2 Electrical Model

The electrical model for the simulation of the dynamic behavior consists of two additional parts beside the FEM model: a stator circuit and a rotor circuit.

3.2.1 Stator Circuit

The three-phase-voltage system is built with two sinusoidal voltage sources with a phase shift of 120° and an amplitude of the line-to-line voltage. The motor has three phases. Every phase consists of a phase resistor, a leakage inductor for the overhanging windings and a voltage source to couple the FEM model to the stator circuit. This circuit can be built in the Electric Circuit physic. An alternative, which leads to the same results but longer solving times, is to define the equations for the three phase currents directly as ordinary differential equations in the ODE and DAE physic without using a circuit.

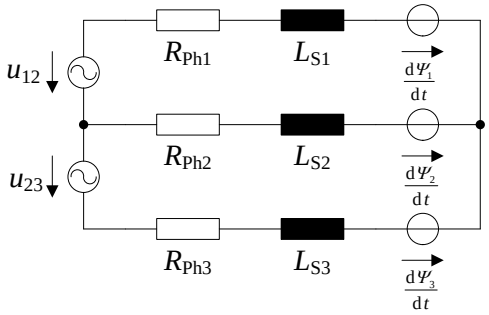

Figure 3. Stator circuit model

The respective phase current in the stator circuit is used in the related Multi Turn Coil Domain in the FEM model. The variable to couple the FEM model to the stator circuit is the time derivative of the field flux linkage, calculated in the respective phase in the FEM model, with

$$\Psi = N\,l_z\left[A_{m(+)}-A_{m(-)}\right] \qquad (3)$$

where N is the number of turns, l_z is the length of the iron and $A_{m(+)}$, $A_{m(-)}$ is the mean value of the one dimensional magnetic vector potential depending on the definition of the current density in the Multi Turn Coil Domain pointing either in $\vec{e}_z$ or $-\vec{e}_z$ direction with

$$A_{\mathrm{m}(+)} = \frac{1}{S_{\mathrm{Slot}}} \int_{S_{i(+)\ \mathrm{Slots}}} A_{\mathrm{z}}\ \mathrm{d}S \qquad (4)$$

and

$$A_{\mathrm{m}(-)} = \frac{1}{S_{\mathrm{Slot}}} \int_{S_{i(-)\ \mathrm{Slots}}} A_{\mathrm{z}}\ \mathrm{d}S\,. \qquad (5)$$

3.2.2 Rotor Circuit

Due to the geometry of rotors for induction motors (Figure 2), the rotor circuit consists of coupled meshes. It is again possible to either use a circuit for them or to define the equations directly as ordinary differential equations.

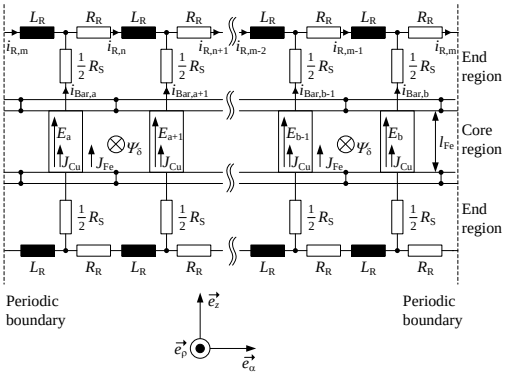

Figure 4. Rotor circuit model for b rotor bars and m meshes.

Figure 4 shows the continuation of Figure 2 for a non-laminated, massive rotor with copper plates to connect the iron in the end rooms. The lumped components in one mesh are six resistors, two inductors and two sources to couple the circuit to the FEM model. The voltage equation between two bars is then given by

$$2L_{\mathrm{R}}\frac{\mathrm{d}i_{\mathrm{R,n}}}{\mathrm{d}t} = -l_{\mathrm{z}}\left[E_{\mathrm{a}} - E_{\mathrm{a+1}}\right] - R_{\mathrm{s}}\left[2i_{\mathrm{R,n}} - i_{\mathrm{R,n-1}} - i_{\mathrm{R,n+1}}\right] - 2R_{\mathrm{R}}i_{\mathrm{R,n}} \qquad (6)$$

The number of meshes m depends on the number of rotor bars b existing in the FEM model and if periodic boundary conditions are used to reduce the motor geometry.

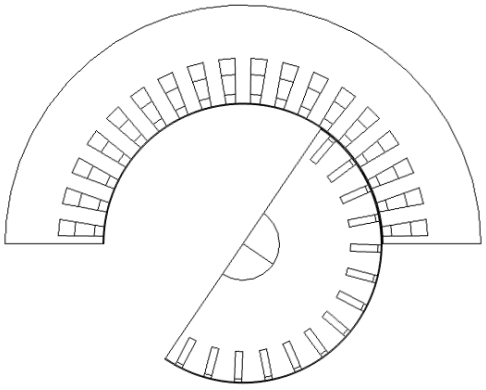

Figure 5. Reduced motor geometry with antiperiodic boundary conditions (2 poles).

If the full model is being simulated, the number of meshes matches the number of bars. If the model is reduced by the use of periodic boundary conditions (Figure 5), there has to be one mesh less than bars. Referring to [2] the solved equation for a rotor bar domain is

$$\vec{J} = \kappa\left[-\frac{\partial \vec{A}}{\partial t} + \vec{E}\right], \qquad (7)$$

which leads, for two dimensions after the surface integration and the first Kirchhoff law for bar number a in Figure 4, to:

$$E_{\mathrm{a}} = \left[\int_{S_{\mathrm{Bar,a}}} \kappa\frac{\partial A_{\mathrm{z}}}{\partial t}\mathrm{d}S + i_{\mathrm{R,n}} - i_{\mathrm{R,n-1}}\right] \cdot \frac{1}{\kappa S_{\mathrm{Bar,a}}} \qquad (8)$$

Equation (8) for bar a and $a+1$ can be used to eliminate the unknown variables E_{a} and $E_{\mathrm{a+1}}$ in equation (6). Defining that equation for the respective mesh as ordinary differential equation with consideration of periodic boundary conditions provides the rotor model. The current in the Single Turn Coil Domain of bar a is then given by

$$i_{\mathrm{Bar,a}} = i_{\mathrm{R,n}} - i_{\mathrm{R,n-1}}. \qquad (9)$$

It is recommended to define the equations directly for a big number of rotor bars, instead of using a circuit, because of the improvable overview of the Electrical Circuit physic.

3.3 Mechanical Model

The rotation velocity is calculated with the equation of motion

$$\vec{T} - \vec{T}_{\mathrm{C}} = I \frac{\mathrm{d}\vec{\omega}_{\mathrm{mech}}}{\mathrm{d}t} \qquad (10)$$

in which I is the momentum of inertia, T_{C} is the counter-torque and T is the inner torque, calculated either with the Maxwell Stress Tensor for two dimensions:

$$\vec{T} = l_{\mathrm{z}} \int_0^{2\pi} \frac{\rho}{\mu_0} B_{\rho}\, B_{\alpha}\, \rho\, \vec{e}_{\mathrm{z}}\, \mathrm{d}\alpha \qquad (11)$$

or the formula of Arkkio, referring to [1]:

$$\vec{T}_{\mathrm{Arkkio}} = \frac{l_{\mathrm{z}}}{\delta} \int_{S_{\mathrm{Airgap}}} \frac{\rho}{\mu_0} B_{\rho}\, B_{\alpha}\, \vec{e}_{\mathrm{z}}\, \mathrm{d}S\,, \qquad (12)$$

where δ is the height of the airgap and B_{ρ} and B_{α} are the absolute values of the $\rho-$ and $\alpha-$components of the magnetic flux density. Equation (10) can be defined as ordinary differential equation to receive the time integral of $\mathrm{d}\,\omega_{\mathrm{mech}} / \mathrm{d}\,t$. The result of the integral can be used as Prescribed Rotational Velocity

$$n = \frac{\omega_{\mathrm{mech}}}{2\pi} \qquad (13)$$

for $[n] = s^{-1}$. An alternative is to integrate equation (10) two times with respect to time and use the result as Prescribed Rotation:

$$\beta = \int \omega_{\mathrm{mech}} \mathrm{d}\,t \qquad (14)$$

In the ODE and DAEs physic, equation (10) should look like

$$f(u, u_{\mathrm{t}}, u_{\mathrm{tt}}, t) = 0 = \frac{\mathrm{d}^2\beta}{\mathrm{d}t^2} - \frac{\vec{T} - \vec{T}_{\mathrm{C}}}{I}\,. \qquad (15)$$

4. Results

For validation there is a program, called DFMZS, basing on [2], which uses the finite differences method and the same theoretical model for the stator and rotor circuits. The simulation results of an induction machine with a massive rotor are compared between COMSOL and DFMZS.

Beside all machine parameters and materials, the voltage phases and the rotor position have to be equal. Calculations with DFMZS were made for constant rotational velocity and standstill.

4.1 Standstill ($n = 0$)

The stationary case for standstill is reached fast and transient procedures can almost be detected in neither the phase current in Figure 6 nor in the bar current in Figure 7.

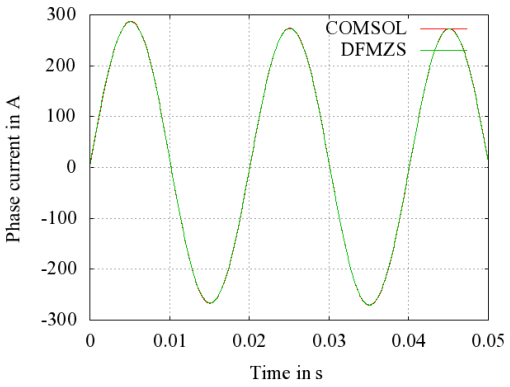

Figure 6. Current in phase one while standstill.

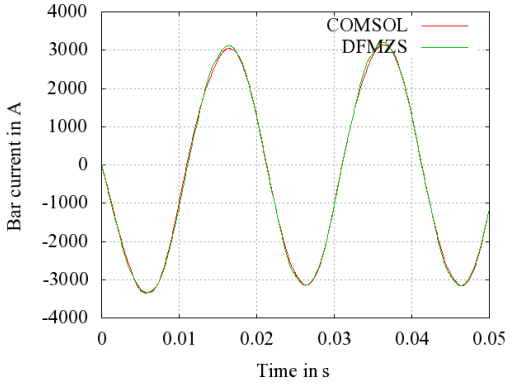

Figure 7. Current in the first rotor bar during stand still.

4.2 Constant rotational velocity

The simulations for a constant velocity **(**here: $n = 2910\ \text{min}^{-1}$**)** other than zero, lead to a transient behavior as seen in Figure 8 for the phase current and in Figure 9 for the bar current.

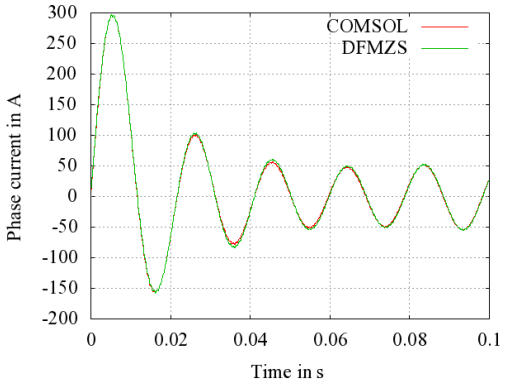

Figure 8. Current in first the phase for constant rotational velocity.

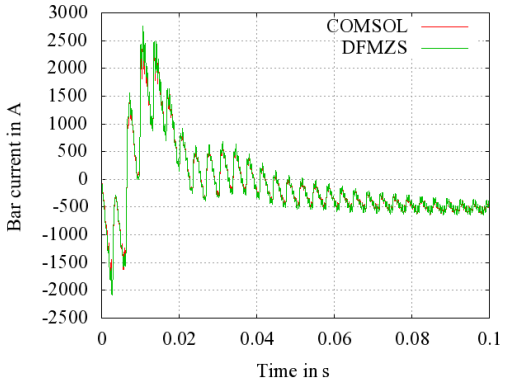

Figure 9. Current in the first rotor bar for constant rotational velocity.

4.3 Start-up

Referring to [1], a fine discretization of the airgap is very important and, if not considered, can lead to big inaccuracies especially for the torque results. Important for the start-up is the inner torque and the momentum of inertia, both being part of the equation of motion. If there are little differences in the calculated rotating speed in two simulations which are to be compared, the rotor positions differ more and more with time and so subsequently do the results of the electrical variables.

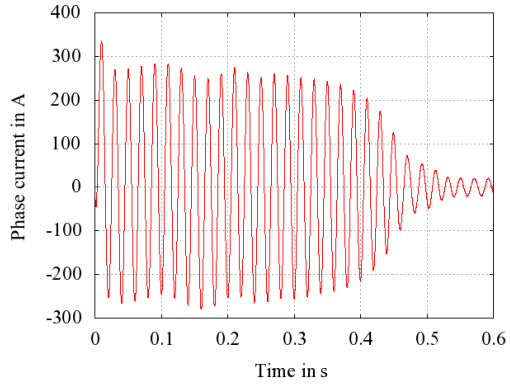

Figure 10. Current in the first phase during start-up.

Figure 10 shows the phase current during the start-up. Typical for induction machines is the much higher phase current while the motor stands still or is running slowly. The faster it rotates, the more the phase current decreases and the more harmonics can be detected in the bar current (Figure 11).

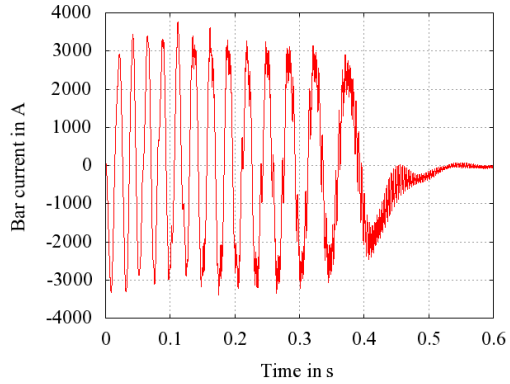

Figure 11. Current in the first rotor bar during start-up.

When the rotor gains speed to the rotating velocity of the magnetic field, the strengths of the induced electrical fields decrease because of the lack of relative movement between the rotating field and the rotor. The bar current drops as a result of this what then again causes a decrease in the torque at the end of the start-up.

Figure 12 shows the time dependent torque, calculated with the Maxwell Stress Tensor. Since this is the dynamical and not the stationary simulation, the torque is rippled.

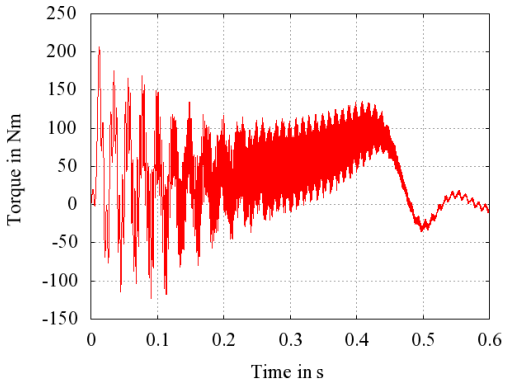

Figure 12. Dynamic torque, calculated with the Maxwell Stress Tensor.

Figure 13 shows the revolutions per minute with respect to time. The ripples in the beginning of the start-up are caused by the big negative torque in the respective moments. The number of poles of the calculated induction machine is two and therefore the rated speed is a little lower than $3000\,\mathrm{min}^{-1}$.

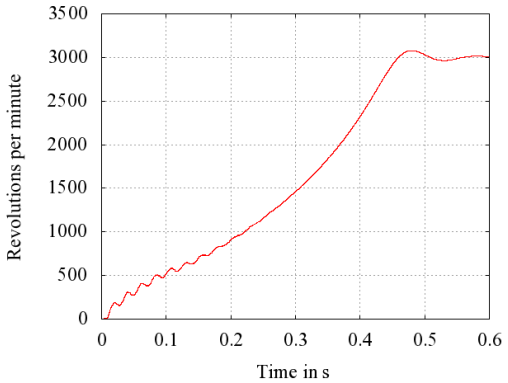

Figure 13. Revolutions per minute with respect to time during the start-up.

6. Conclusions

Coupling different kind of physic interfaces like Electric Circuit and Rotating Machinery within the COMSOL model allowed to reduce the three dimensional model of an induction machine to two dimensions without neglecting electrical effects, which are relevant for the dynamical behavior. As shown in chapter 4, the simulation results of this COMSOL model accord well with the results of the program DFMZS which was validated in [2].

The next step is to use the experience acquired with this model to calculate the dynamical behavior of synchronous motors, beside improving this ASM model especially in terms of solving times.

7. References

[1] Arkkio A., Analysis of Induction Motors Based on the Numerical Solution of the Magnetic Field and Circuit Equations, *Acta Polytechnica Scandinavica, Electrical Engineering*, Series No.59, Helsinki 1987

[2] Gottkehaskamp R., Nichtlineare Berechnung von Asynchronmaschinen mit massiveisernem Rotor und zusätzlichem Käfig im stationären und transienten Zustand mittels Finiter Differenzen und Zeitschrittrechnung, *VDI-Verlag Fortschritt-Berichte*, VDI Series No.131, Dortmund 1993